# Crystal Orientation in Injection Molding of Talc-Filled Polypropylene

MITSUYOSHI FUJIYAMA* and TETSUO WAKINO

Polymer Development Laboratory, Tokuyama Soda Co., Ltd., Tokuyama-shi, Yamaguchi-ken 745, Japan

SYNOPSIS

The crystal orientation in injection molding of talc-filled polypropylene has been studied by means of polarizing microscopy and X-ray diffraction measurements. The plate planes of talc particles are aligned parallel to the surface of injection molding. The $c$- and $a^*$-axes of polypropylene crystals are bimodally oriented to the flow direction, and the $b$-axes are oriented to the thickness direction. Namely, the crystals in the injection molding of talc-filled polypropylene show a kind of uniplanar-axial orientation according to the classification of Heffelfinger and Burton. The degree of the bimodal orientation of $c$- and $a^*$-axes decreases toward the interior of the injection molding. The $b$-axis orientation is strong throughout the thickness direction, although it is a little weaker at the surface skin and central regions. This peculiar crystal orientation originates from the flaky shape and crystallization nucleation ability of talc particles. In a mold cavity, talc particles are aligned parallel to the cavity wall by the action of flow, and crystallization progresses, with the (040) plane of polypropylene crystal piling on the plate planes of talc particles and the $b$-axis, which is the growth direction of polypropylene crystal, being aligned to the thickness and cooling direction of injection molding. The crystal orientation in injection molding of unfilled polypropylene is basically similar to that of talc-filled polypropylene, although the $b$-axis orientation to the thickness direction is much weaker.

## INTRODUCTION

In injection molding of plastics, since a molten resin flows into a cold mold cavity at high speed, where it is solidified, orientation of molecular chains occurs, significantly affecting product properties such as mechanical and optical properties. In the case of injection molding of semicrystalline polymers, since the molecular chains are crystallized under a stress, orientation of crystallites occurs. Several studies have so far been done on the orientation state of crystals in injection-molded semicrystalline polymers.[1-12]

Clark[2] found from X-ray diffraction measurement that the skin layer in injection-molded polypropylene has a mixed $c$-axis and $a^*$-axis orientation, which he called bimodal; he explained its formation by assuming that the $c$-axis-oriented component was formed first, and that the $a^*$-axis component was formed by epitaxial overgrowth on the $c$-axis-oriented substrate.

Kantz et al.[4] made X-ray diffraction measurements on the skin layer in injection-molded polypropylene from various directions and found that crystallites are biaxially oriented to MD and that the tensile yield strength and mold shrinkage in MD were higher as the skin layer was thicker.

Mencik and Fitchmun[5] found, from polarizing microscopy and X-ray diffraction measurement, that injection-molded polypropylene is composed of five layers, whose thickness changed according to molding conditions. They conjectured that the first layer at the surface region had a weak mixed $c$-axis and $a^*$-axis orientation, the second layer had an $a^*$-axis orientation, the third layer had a strong mixed $c$-axis and $a^*$-axis orientation, the fourth layer was composed of a mixture of isotropic monoclinic crystals and uniaxially oriented crystals of the other type, and the core layer at the central region was

* To whom correspondence should be addressed.

Journal of Applied Polymer Science, Vol. 42, 9-20 (1991)
 CCC 0021-8995/91/010009-12$04.00

unoriented. They explained the formation of the mixed $c$-axis and $a^*$-axis orientation in the third layer by assuming that lath-like crystallites whose $a^*$-axes oriented to MD were formed first and the $c$-axis-oriented component was formed by unfolding the molecular chains of the $a^*$-axis-oriented component by the action of shearing force.

Clark and Spruiell[9] proposed a structural model of injection-molded polypropylene. In this model, lamellae whose $c$-axes are oriented to MD and whose plate planes are normal to MD are connected by tie molecules, and small and imperfect lamellae whose $a^*$-axes are oriented to MD pile epitaxially between the $c$-axis-oriented lamellae. The small and imperfect $a^*$-axis-oriented lamellae act as a morphological plasticizer, which they considered to be the cause of good hinge of injection-molded polypropylene.

Experiments performed by Fujiyama and his colleagues[7,12] showed, with polarizing microscopy, measurements of wide-angle X-ray diffraction, small-angle X-ray scattering, melting behavior, density, and dynamic viscoelasticity, and the tensile test of an injection-molded polypropylene, that the skin layer is composed of shishkebab-like main skeleton structure whose axis is parallel to MD piled epitaxially with $a^*$-axis-oriented imperfect lamellar substructure, and the core layer is composed of spherulites (the crystals in which have weak $c$-axis and $a^*$-axis orientations to MD).

It is well known that, when polypropylene is filled with talc, its rigidity, heat distortion temperature, tensile and flexural strengths, and thermal conductivity increase, and its thermal expansion coefficient, mold shrinkage, and impact strength decrease because of flaky shape and crystallization nucleation ability of talc particles.[13] Talc-filled polypropylenes are widely used as parts of automobiles, electrical machinery and appliances, and industrial goods, particularly owing to their excellent heat-resistant rigidity.

The authors studied the crystalline structure of injection moldings of talc-filled polypropylenes and found that they showed a peculiar crystal orientation, which is reported in this paper.

## EXPERIMENTAL

### Samples

As polypropylene, homo-polypropylene powder was used (Grade PN120, Tokuyama Soda Co., Ltd., with a melt flow index (MFI) = 2 dg/min). As fillers, Crown Talc Z (TC; Matsumura Industry Co., Ltd., average diameter, 10 $\mu$m) and Stavigot 15A (CC; a precipitated calcium carbonate produced by Shiraishi Industry Co., Ltd., surface-treated with an aliphatic acid; average diameter, 0.2 $\mu$m) were used.

As crystallization nucleators, *p-tert*-dibutyl-benzoic acid monohydroxy aluminum (BA; Shell Chemical Co., Ltd.) and Gelall MD (GA; *p*-dimethyl-benzylidene sorbitol, New Japan Chemical Co., Ltd.) were used. Figure 1 shows transmission electron micrographs of these fillers and nucleators.

The polypropylene powder was mixed with fixed amount of fillers or nucleators for 5 min in a 100 L Supermixer, extruded by a CCM extruder with a vent at a kneader temperature of 190°C and an extruder temperature of 220°C into a strand which was cut into pellets of about 3 mm size by an automatic cutter. Filler contents were 0, 0.5, 10, 20, 30, 40, and 60 wt %, and nucleator content was 0.5 wt %. Hereinafter, the sample with filler content of 0 wt % is called PP, the sample with TC content of 0.5 wt % is called TC-0.5, the sample with TC content of 10 wt % is called TC-10, and so on. Likewise, the sample with CC content of 0.5 wt % is called CC-0.5, the sample with CC content of 10 wt % is called CC-10, and so on. The sample with BA content of 0.5 wt % is called BA-0.5, and the sample with GA content of 0.5 wt % is called GA-0.5.

Figure 2 shows the dependence of crystallization temperatures $T_c$ of filled polypropylenes on the filler content which was measured by a differential scanning calorimeter (DSC). Figure 3 shows the dependence of $T_c$ of nucleator-added polypropylenes on the cooling rate. A sheet 0.3 mm thick was molded on a hot plate. It was put into a sample pan, and, after it was melted in the furnace of DSC in a nitrogen atmosphere at 230°C for 10 min, it was cooled at various rates. The peak temperature of the exothermic curve was taken as $T_c$. It is seen from Figure 2 that $T_c$ increases by about 10°C by the filling of 0.5 wt % TC, and it gradually increases with increasing TC content after that. $T_c$ increases by 1–2°C by the filling of CC independent of CC content. Figure 3 shows that the crystallization nucleation ability is notable in the order of GA > BA > TC > CC.

### Injection Molding

Flexural test specimens (ASTM D790) were injection-molded using an 8 oz Nikko Ankerwerk V22A-120 type reciprocating-screw injection molding machine. The shape of the test specimen is shown in Figure 4. A polymer reservoir was provided to make resin flow in the specimen uniform. Since the cylinder temperature among molding conditions most

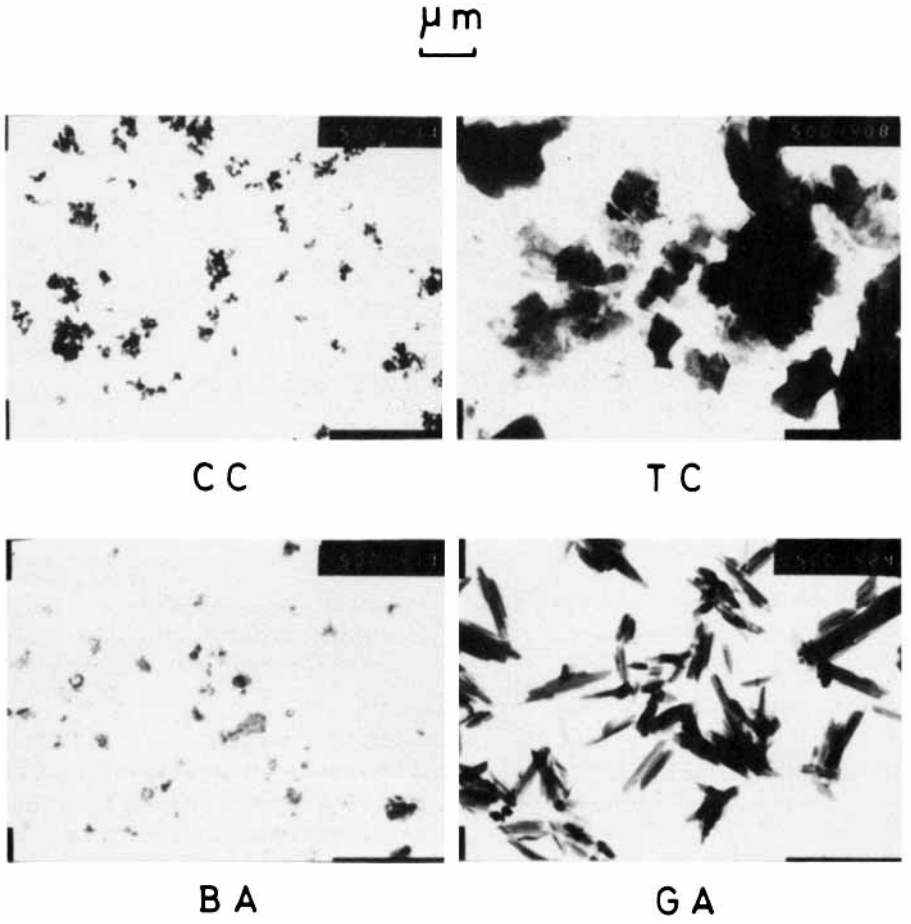


**Figure 1** Transmission electron micrographs of fillers and crystallization nucleators.

strongly affects the degree of orientation and mechanical properties of the molded article,[14] injection molding was carried out, varying only the cylinder temperature and keeping all other conditions constant. The injection molding conditions are shown in Table I. The cylinder temperatures were represented by the temperature of the metering zone (MH3) at the extreme end.

## Structural Analyses

Thin sections about 100 μm thick were sliced from the central parts of the flexural specimens perpendicular to the flow direction (MD) with a microtome, and their crystalline textures were observed with a polarizing microscope (Olympus PM-6) under a magnification of 20×. Thin sections about 20 μm thick were sliced similarly and the dispersion states of fillers were observed under a magnification of 100×.

2θ-scan diffraction curves were measured at the central parts of the flexural specimens with a Rigaku Denki RU-200 diffractometer with Ni-filtered Cu-Kα radiation using a rotating specimen table. Owing to the absorption of X-ray by the filler, good diffraction curves could be obtained only at TC contents not exceeding 30 wt % and at CC contents not exceeding 10 wt %.

For PP and TC-10 specimens molded at a cylinder temperature of 240°C, wide-angle X-ray diffraction patterns were taken at the central parts from various directions with the same apparatus under a sample-to-film distance of 45 mm. The diffractions of through view (THRU) were taken on the specimens of original thickness. The diffractions of edge view (EDGE) and end view (END) were taken on sections about 1 mm thick, cut out from the central parts of specimens perpendicular to the surface and parallel to MD and transverse direction (TD), respectively. For the same samples as used for taking the photographs, the 2θ-scan diffraction curves of THRU, EDGE, and END were measured using the rotating specimen table.

For PP and TC-10 specimens molded at a cylinder temperature of 240°C, thin sections, about 0.3 mm thick, were sliced successively from the surface to

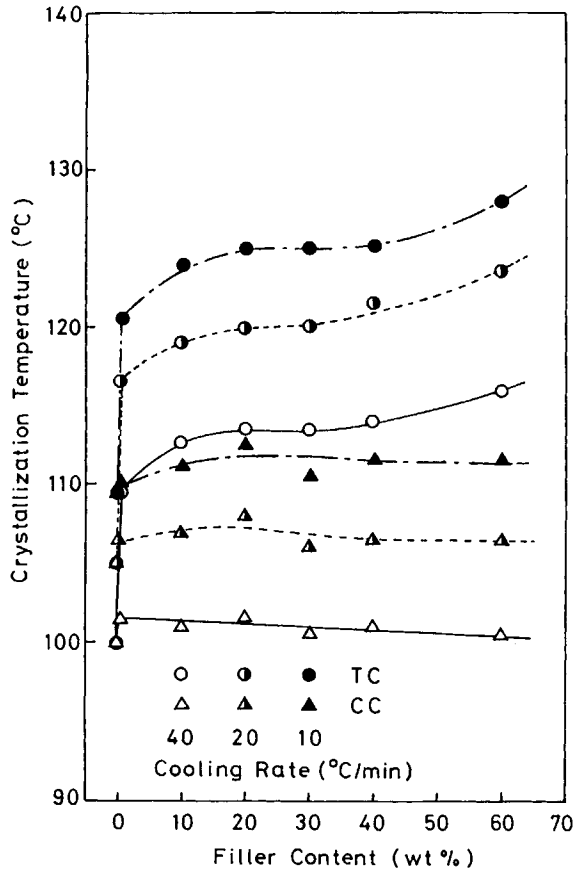


**Figure 2** Dependence of crystallization temperatures on filler content.

the center parallel to the surface at the central parts of the specimens with the microtome. For these sections, $2\theta$-scan curves in THRU were measured using the rotating specimen table. Also, the azimuthal scan curves of the (110) and (040) planes in THRU were measured. The changes of crystal orientation state in the thickness direction of the specimens were then studied.

## RESULTS

Figure 5 shows, as an example, the $2\theta$-scan diffraction curves, measured using the rotating specimen table, of specimens molded from TC-filled polypropylenes at a cylinder temperature of 240°C. It can be seen from Figure 5 that the reflection intensities of the (040) and (130) planes, particularly of the (040) plane, decrease significantly with the filling of TC. The decrease of the reflection intensities of the (040) and (130) planes is already noticeable with

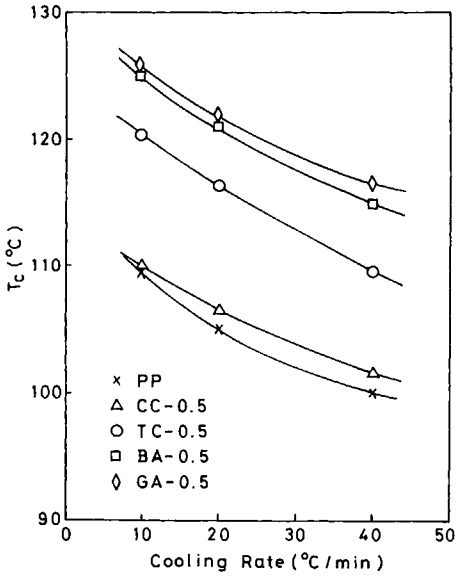


**Figure 3** Dependence of crystallization temperatures of nucleator-added polypropylenes on cooling rate.

a very small amount of TC filling of 0.5 wt %, and it becomes more noticeable with increasing TC content. This means that the (040) planes are parallel to the specimen surface, or that the *b*-axes are perpendicular to it. In order to evaluate this degree, the ratio of the intensity of the (040) reflection, $I(040)$, to that of the (110) reflection, $I(110)$, is used. The baseline which is used for the determination of the crystallinity according to Weidinger and Hermans' method[15] was used for the determination of reflection intensities.

Figure 6 shows the dependence of the ratio $I(040)/I(110)$ on filler content. Although CC filling scarcely changes the ratio, TC filling abruptly decreases the ratio. Figure 7 shows the variations of the intensity ratios of the nucleator-added polypropylenes with the cylinder temperature. In contrast to TC-0.5 which shows very small intensity ratios, other nucleators scarcely affect the ratio. Since the nucleation abilities of BA and GA are stronger than that of TC, the decrease of the intensity ratio by TC

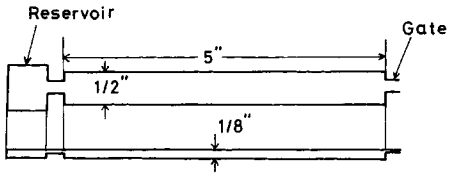


**Figure 4** Shape of test specimen.

**Table I Injection Molding Conditions**

| Expt. No. | Cylinder Temperature (°C) | | | | Injection Pressure (kg/cm²) | Injection Speed (cc/s) | Mold Temperature (°C) | Cooling Time (s) |
|---|---|---|---|---|---|---|---|---|
| | MH1[a] | MH2[b] | MH3[c] | DH[d] | | | | |
| 1 | 160 | 190 | 200 | 190 | 500 | 13.5 | 40 | 40 |
| 2 | 160 | 220 | 240 | 220 | 500 | 13.5 | 40 | 40 |
| 3 | 160 | 250 | 280 | 250 | 500 | 13.5 | 40 | 40 |
| 4 | 160 | 280 | 320 | 280 | 500 | 13.5 | 40 | 40 |

[a] Feed Zone.
[b] Compression Zone.
[c] Metering Zone.
[d] Die Head.

filling cannot be elucidated from the viewpoint of nucleation ability alone.

If *b*-axes are aligned perpendicular to the surface of injection molding of talc-filled polypropylene, the reflection intensity of the (040) plane must be strong in the diffractions of EDGE and END. Figure 8 shows $2\theta$-scan diffraction curves taken, using the rotating specimen table, from the various directions of TC-10 specimen molded at a cylinder temperature of 240°C. As expected, the (040) reflections of EDGE and END are very strong. In addition, considering that the cleavage plane of talc is the (002) plane, the fact that the talc (002) reflection at $2\theta = 9.4°$ is not observed in THRU and that it is strong in EDGE and END means that talc particles are aligned parallel to the specimen surface. Figure 9 shows the results for PP. Although PP shows a similar tendency to that of TC-10, the degree is very weak.

Figure 10 shows wide-angle X-ray diffraction patterns taken from various directions. As for PP, THRU shows a mixed *c*-axis and *a**-axis orientation to MD, and EDGE and END show that the *b*-axes are weakly oriented to the plane perpendicular to MD and TD, namely to the normal direction (ND). Meanwhile, as for TC-10, THRU shows a mixed *c*-axis and *a**-axis orientation to MD, as in the case of PP, and EDGE and END show that the (040) reflection is concentrated on the equatorial direction (ND), which means that the *b*-axes are strongly oriented to the plane perpendicular to MD and TD, namely to ND. In addition, the (110) and (130) re-

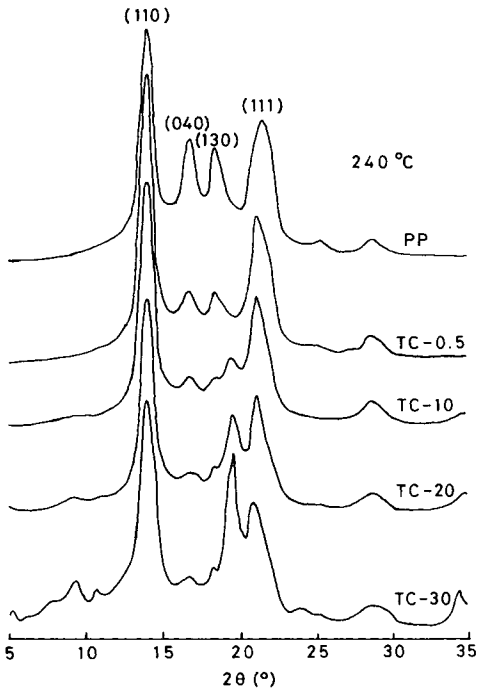


**Figure 5** Variation of $2\theta$-scan curve in THRU with talc content. Measured using a rotating specimen table.

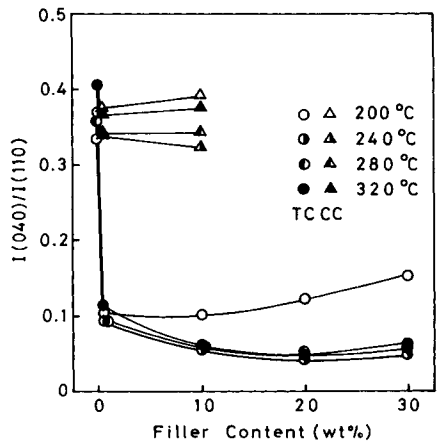


**Figure 6** Dependence of reflection intensity ratios $I(040)/I(110)$ on filler content (THRU).

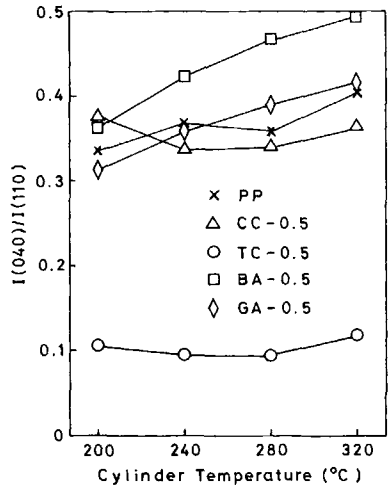


**Figure 7** Dependence of reflection intensity ratios of nucleator-added polypropylenes, $I(040)/I(110)$, on cylinder temperature (THRU).

flections are concentrated on the first layer line, which means that the $a^*$-axes are oriented to MD and TD.

As mentioned above, the $c$-axes and $a^*$-axes are mixedly oriented to MD and the $b$-axes are oriented to ND in injection-molded TC-10 specimen. Although the injection-molded PP specimen shows similar orientation to that of TC-10 specimen, its degree of $b$-axis orientation to ND is much weaker.

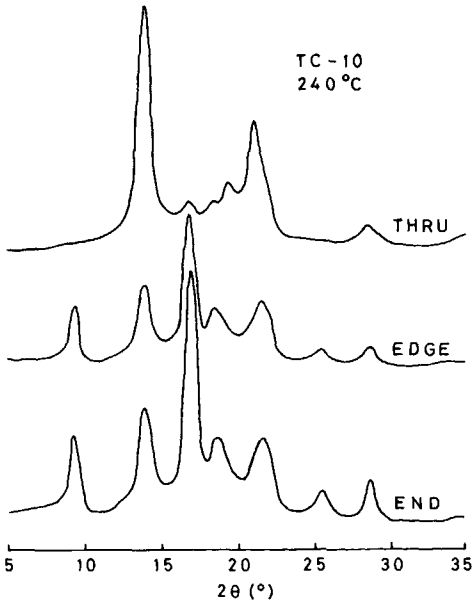


**Figure 8** $2\theta$-scan curves measured from various directions. TC-10, cylinder temperature; 240°C.

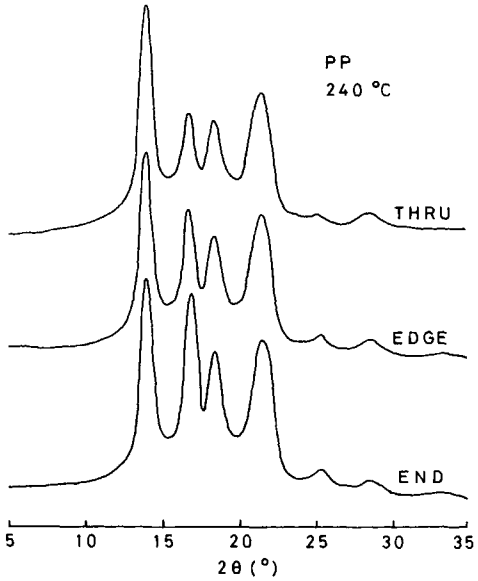


**Figure 9** $2\theta$-scan curves measured from various directions. PP, cylinder temperature; 240°C.

Next, we study the variation of crystal orientation state in injection-molded specimens in the thickness direction. Figure 11 shows, as an example, the polarized micrograph of a thin section sliced normal to MD, from TC-10 specimen molded at a cylinder temperature of 240°C. A clear skin/core structure can be observed. The thickness of the skin layer in this case is 0.18 mm. The skin/core structure could be observed in TC and CC specimens whose filler contents were up to 40 wt %. We could not discriminate between the skin and core layers in BA-0.5 and GA-0.5 specimens. The thickness of the skin layer increases with decreasing the cylinder temperature and increasing the filler content.

Figure 12 shows polarized micrographs of TC-10 specimen molded at a cylinder temperature of 240°C taken at a magnification of 100×. Although the orientation of talc particles is disordered a little around the center region, they are aligned parallel to the specimen surface throughout almost all regions in the thickness direction. This fact is in good agreement with the assumption from the wide-angle X-ray diffraction in Figure 8. It is not obvious whether transcrystals are formed around talc particles or not.

Figure 13 shows the variations of the intensity ratio $I(040)/I(110)$ in the thickness direction. In this figure, $H$ is a half of the thickness of specimen and $y$ is the distance from the center. As for the PP specimen, the ratio is a little large at the point nearest the surface, about half of which consists of the skin layer, decreases once, and increases toward the

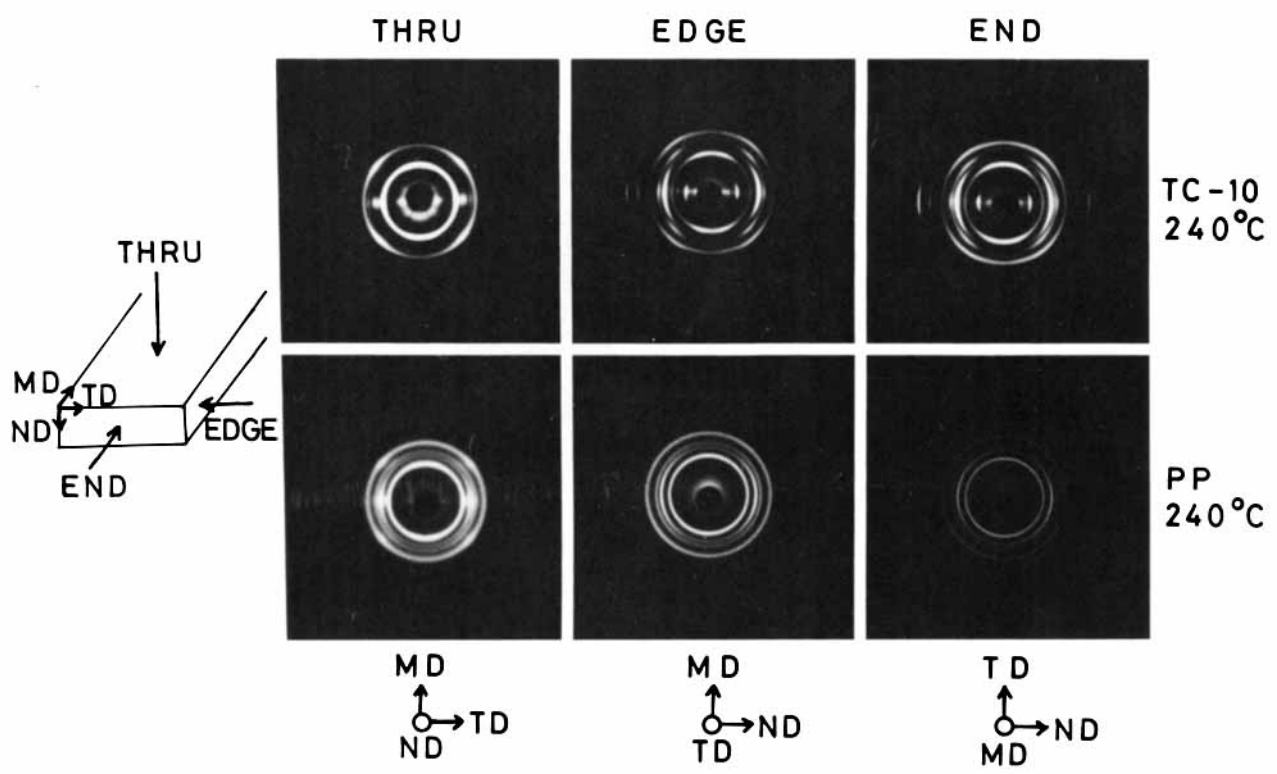


**Figure 10** Wide-angle X-ray diffraction patterns taken from various directions.

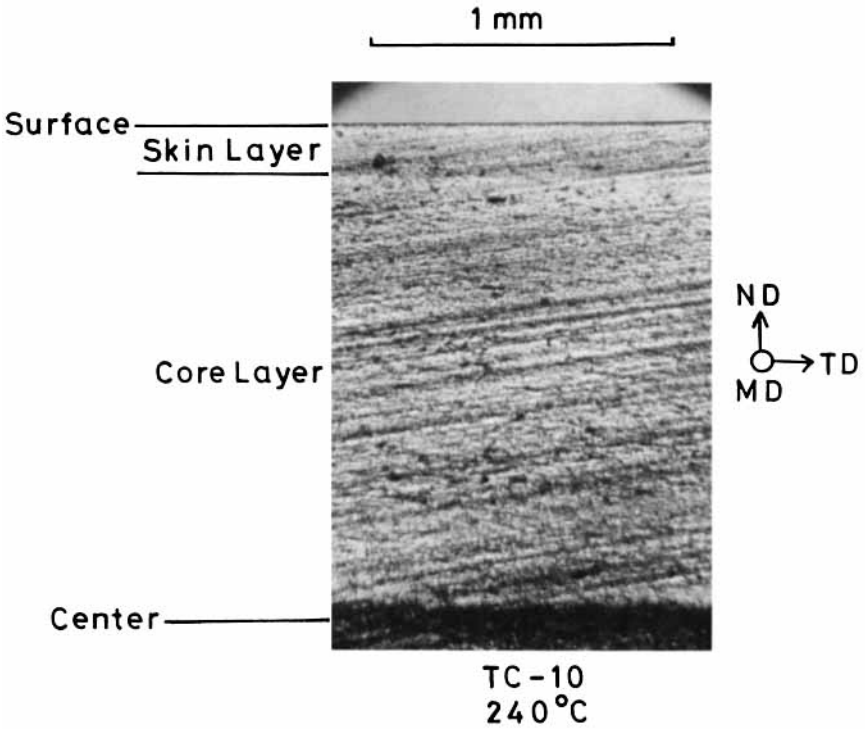


**Figure 11** Polarized micrograph (20×) of thin section sliced perpendicular to flow direction. TC-10, cylinder temperature; 240°C.

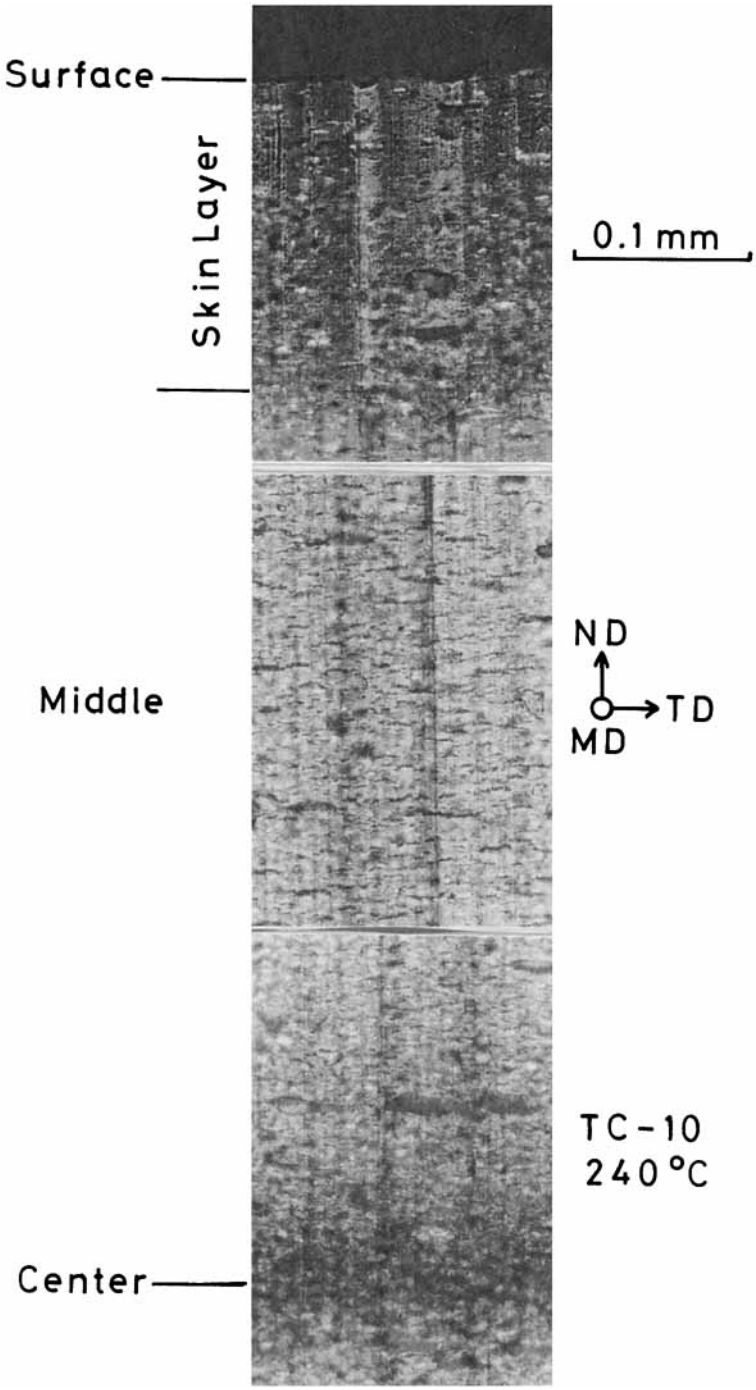


**Figure 12** Polarized micrographs (100×) of thin section sliced perpendicular to flow direction. TC-10, cylinder temperature; 240°C.

center. On the other hand, for TC-10 specimen, the ratio is a little large at the point nearest the surface, about half of which consists of the skin layer, decreases toward the center, and increases a little at around the center. The TC-10 specimen shows much smaller ratios than the PP specimen throughout the whole range. From this, it can be said that the orientation of *b*-axes to ND in TC-10 specimen is strong throughout the whole range in the thickness direction, although it is a little weak at the skin and

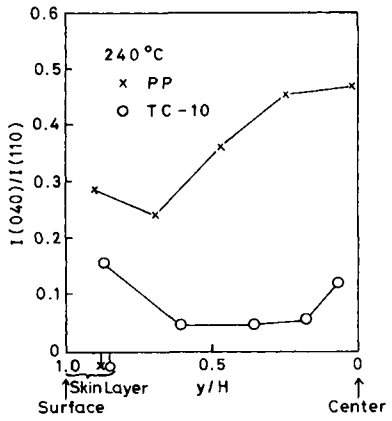


**Figure 13** Variations of reflection intensity ratios $I(040)/I(110)$ in thickness direction.

center regions. On the other hand, the orientation of *b*-axes to ND in the PP specimen is generally weak and decreases toward the interior.

Figure 14 shows the variations, in the thickness direction, of the azimuthal scan curves of PP specimen molded at a cylinder temperature of 240°C. As for the (110) reflection azimuthal scan, the sample at $y/H = 0.896$ which contains the skin layer in its

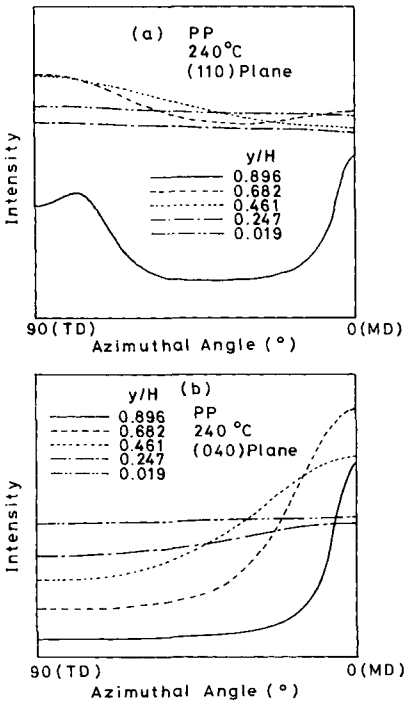


**Figure 14** Variations of (a) (110) plane and (b) (040) plane azimuthal scan curves in thickness direction. PP, cylinder temperature; 240°C, THRU.

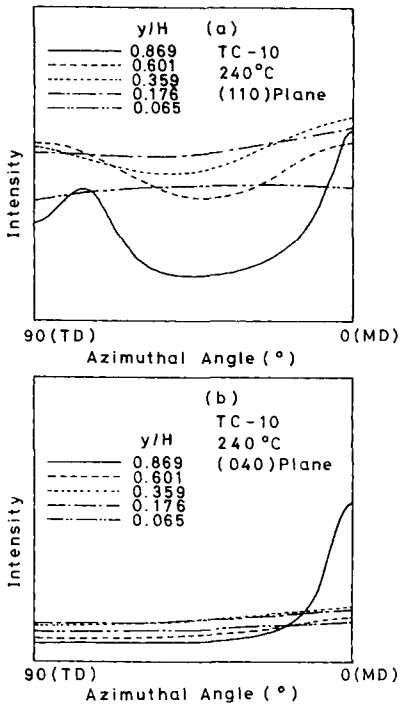


**Figure 15** Variations of (a) (110) plane and (b) (040) plane azimuthal scan curves in thickness direction. TC-10, cylinder temperature; 240°C, THRU.

about half shows a mixed *c*-axis and *a**-axis orientation to MD. The samples at $y/H = 0.682$ and 0.461 show weak *a**-axis orientations to MD. The samples at around the center at $y/H = 0.247$ and 0.019 show almost random orientation. As for the (040) reflection azimuthal scan, the orientation of *b*-axes to the plane perpendicular to MD becomes weaker as $y/H$ decreases or going to the interior.

Figure 15 shows the results of TC-10 specimen. As for the (110) reflection azimuthal scan, the sample at $y/H = 0.869$ which contains the skin layer in its about half shows a strong mixed *c*-axis and *a**-axis orientation to MD. This orientation weakens as $y/H$ decreases or going to the interior and almost random at $y/H = 0.065$. On the other hand, as for the (040) reflection azimuthal scan, although the sample at $y/H = 0.869$ which contains the skin layer in its about half shows the *b*-axis orientation to the plane perpendicular to MD, the inner samples show much weaker *b*-axis orientations. In comparison with the PP specimen, the (040) reflections are weak for the (110) reflection intensities throughout the whole range in the thickness direction. These are the results of THRU. If EDGE and END are measured, it is conjectured that the (040) reflections must show strong peaks at an azimuthal angle of

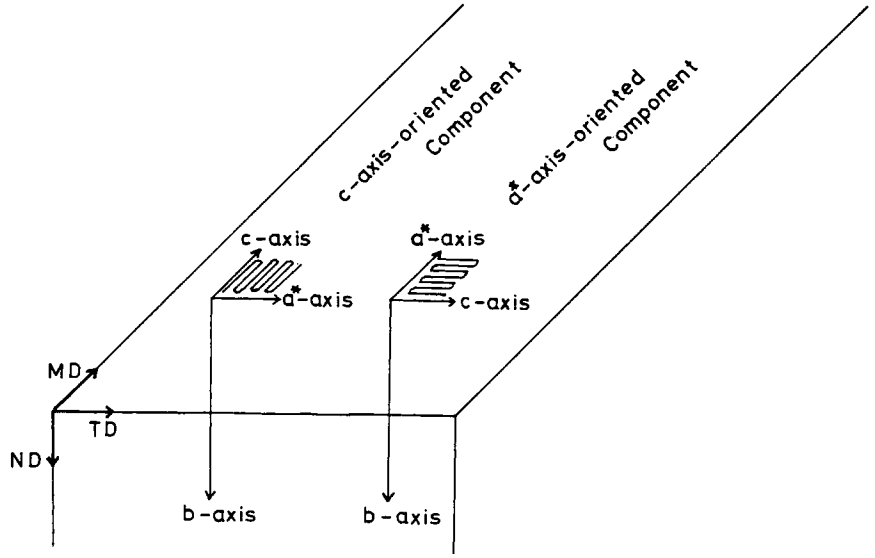


**Figure 16** Crystal orientation state in injection molding of talc-filled polypropylene.

0°. The (040) reflection of the sample at $y/H = 0.869$ which contains the skin layer in its about half shows a considerably strong reflection at an azimuthal angle of 0°. This is assumed to be because considerable amounts of the *b*-axes are oriented to TD. This agrees with the fact that the ratio $I(040)/I(110)$ at the part nearest the specimen surface is considerably large in Figure 13. In comparison to this, it is conjectured that there is almost no *b*-axis oriented to TD in the inner parts and most *b*-axes are oriented to ND.

## DISCUSSION

Summarizing the above results, the *c*-axes and *a**-axes are mixedly oriented to flow direction (MD), and the *b*-axes are oriented to the normal direction (ND), in injection molding of talc-filled polypropylene. Namely, according to the classification of Heffelfinger and Burton,[17] it shows a kind of uniplanar-axial orientation. This situation is represented in Figure 16. In the skin layer, the orientation of *b*-axes to ND is a little weak, and there is a little rotation of *b*-axes around MD. The mixed *c*-axis and *a**-axis orientation to MD decreases toward the interior of specimen. Although injection-molded polypropylene basically shows a similar crystal orientation to that shown in Figure 16, the degree of orientation is much weaker than that of a talc-filled one. Namely, in the first place, the degree of *b*-axis orientation to ND is very weak, and it is conjectured that most *b*-axes rotate around MD. Next, although the mixed *c*-axis and *a**-axis orientation to MD is strong in the skin layer, there is small component whose *a**-axes are oriented to MD in the next inner region, and almost no orientation is observed in the inmost central region. These results concerning the crystal orientation state in injection-molded polypropylene agree with the results of our previous paper.[12]

The growth mechanism of polypropylene crystal in which the fold plane is the (040) plane, the growth axis is the *a**-axis, and the growth direction is the *b*-axis direction, is favorable to the formation of the crystal orientation state in Figure 16. Namely, in injection molding, the resin injected into a cavity is cooled more rapidly at the part nearer the surface, and crystallization progresses from the surface to the interior. Consequently, it is natural that crystallization progresses so as the *b*-axes, which are the growth direction, come to be perpendicular to the surface. It is conjectured that the orientation of talc particles promotes this tendency. As shown in Figure 12, talc particles are oriented to the specimen surface throughout almost all regions in the thickness direction.

It is well known that polypropylene transcrystallizes under the existence of mica,[19–22] glass fiber,[23–27] carbon fiber,[28–30] organic fiber,[31,32] and alkaline halides.[33] The transcrystallization is also observed in the injection moldings of polypropylenes which contain mica,[20,21] glass fiber,[24–27] and carbon fiber.[29] Although it is known that talc is a crystal-

lization nucleator of polypropylene,[34-36] for some unknown reason, transcrystallization of polypropylene on it has not been reported.

Although no evidence of transcrystallization of polypropylene on talc particles is seen in Figure 12, it is conjectured that crystals grow on talc particles as nuclei. It may be said from the data in Figures 12 and 16 that polypropylene crystals grow with their *b*-axes perpendicular to the plate planes of talc particles. Namely, it is conjectured that the (040) planes of polypropylene crystals are piled on the plate planes of talc particles. Talc belongs to the monoclinic crystallographic system and its unit cell has a dimension of $a = 5.26$ Å, $b = 9.10$ Å, $c = 18.81$ Å, and $\beta = 100°\ 00'$[37] and its cleavage plane is the (002) plane. On the other hand, polypropylene also belongs to the monoclinic system and its unit cell has a dimension of $a = 6.65$ Å, $b = 20.96$ Å, $c = 6.50$ Å and $\beta = 99°\ 20'$.[38] From these values, it is seen that there is no lattice matching between the cleavage plane of talc and the (040) plane of polypropylene. Although Rybnikář[39] and Wittmann and Lotz[40,41] reported that there is a lattice matching between polyethylene and talc crystals, the lattice matching is not necessarily needed for epitaxial crystallization, according to Koutsky et al.[42] A necessary condition for transcrystallization is a stress concentration, according to Gray[23] and Misra,[25] and a concentration of melt orientation according to Campbell and White.[26] Since flaky particles such as talc and mica, and fibrous materials such as glass and carbon fibers, easily cause the concentration of stress or melt orientation in injection molding of plastics containing such materials, the existence of such materials is favorable for the transcrystallization of the plastics. In the case of injection molding of talc-filled polypropylene in this experiment, transcrystallization is not clearly seen in Figure 12. However, in consideration of the above-mentioned points, it is conjectured that the (040) planes of polypropylene crystals pile epitaxially on the plate planes (cleavage planes) of talc particles which have been aligned parallel to the cavity wall by the action of flow and crystallization proceeds in the *b*-axis direction which is the growth direction of polypropylene crystal. At this time, the agreement of cooling direction with crystal growth direction is favorable for the crystallization of polypropylene. In this way, the existence of talc particles promotes the orientation of the *b*-axes in injection-molded polypropylene which contains them to its thickness direction. The fact that the addition of even very small amount (0.5 wt %) of talc shows such remarkable effect is because crystal growth initiates at the places where talc particles exist and propagates to the whole. Although talc has a strong nucleation effect on the crystallization of polypropylene, as shown in Figures 2 and 3, the crystal orientation mentioned above is not due solely to the nucleation effect. This is obvious from the fact that the intensity ratio $I(040)/I(110)$ of injection moldings of BA-0.5 and GA-0.5, which are polypropylenes added with BA and GA, whose nucleation effects are stronger than that of talc, differ little from that of PP. It is conjectured that the flaky shape (of talc), or both the flaky shape and the crystallization nucleation effect together, constitute the necessary condition.

## CONCLUSIONS

In the injection molding of talc-filled polypropylene, polypropylene crystals show a peculiar orientation in which the *c*- and *a**-axes are bimodally oriented to the flow direction, and *b*-axes are oriented to the thickness direction.

This peculiar crystal orientation originates from the flaky shape and crystallization nucleation ability of talc particles. In a mold cavity, talc particles are aligned parallel to the cavity wall by the action of flow, and crystallization proceeds, with the (040) plane of polypropylene crystal piling on the plate planes of talc particles and the *b*-axis being aligned parallel to the thickness and cooling direction of injection molding.

The crystal orientation in injection molding of unfilled polypropylene is basically similar to that of talc-filled polypropylene, although the *b*-axis orientation to the thickness direction is much weaker.

## REFERENCES

1. E. S. Clark, *SPE J.*, **23**(7), 46 (July, 1967).
2. E. S. Clark, Paper presented at Meeting of the American Physical Society, Dallas, 1970.
3. W. Heckmann and G. Spilgies, *Kolloid-Z. Z. Polym.*, **250**, 1150 (1972).
4. M. R. Kantz, H. D. Newman, Jr., and F. H. Stigale, *J. Appl. Polym. Sci.*, **16**, 1249 (1972).
5. Z. Mencik and D. R. Fitchmun, *J. Polym. Sci. Polym. Phys. Ed.*, **11**, 973 (1973).
6. T. W. Owen and D. Hull, *Plast. Polym.*, **42**(157), 19 (1974).
7. M. Fujiyama, *Kobunshi Ronbunshu*, **32**, 411 (1975).
8. B. Heise, *Kolloid Polym. Sci.*, **254**, 279 (1976).
9. E. S. Clark and J. E. Spruiell, *Polym. Eng. Sci.*, **16**, 176 (1976).

10. W. Woebcken and B. Heise, *Kunststoffe*, **68,** 99 (1978).
11. B. Heise and M. Pietralla, *Progr. Colloid Polym. Sci.*, **66,** 113 (1979).
12. M. Fujiyama, T. Wakino, and Y. Kawasaki, *J. Appl. Polym. Sci.*, **35,** 29 (1988).
13. J. Sveda and R. Evanzin, *Int. Polym. Sci. Technol.*, **11**(7), T/4 (1984).
14. M. Fujiyama and S. Kimura, *Kobunshi Ronbunshu*, **32,** 581 (1975).
15. W. Weidinger and P. H. Hermans, *Makromol. Chem.*, **50,** 98 (1961).
16. M. Fujiyama, Y. Kawasaki, and T. Wakino, *J. Soc. Rheol. Jpn.*, **15,** 191 (1987).
17. C. J. Heffelfinger and R. L. Burton, *J. Polym. Sci.*, **47,** 289 (1960).
18. M. Kojima, *J. Polym. Sci. A-2*, **5,** 597 (1967).
19. A. J. Lovinger, *J. Polym. Sci. Polym. Phys. Ed.*, **21,** 97 (1983).
20. A Garton, S. W. Kim and D. M. Wiles, *J. Polym. Sci. Polym. Lett. Ed.*, **20,** 273 (1982).
21. S. F. Xavier and Y. N. Sharma, *Angew. Makromol. Chem.*, **127,** 145 (1984).
22. S. F. Xavier and Y. N. Sharma, *Polym. Compos.*, **7,** 42 (1986).
23. D. G. Gray, *J. Polym. Sci. Polym. Lett. Ed.*, **12,** 645 (1974).
24. S. F. Xavier, D. Tyagi, and A. Misra, *Polym. Compos.*, **3,** 88 (1982).
25. A. Misra, B. L. Deopura, S. Xavier, F. D. Hartley, and R. H. Peters, *Angew. Makromol. Chem.*, **113,** 113 (1983).
26. D. Campbell and J. R. White, *Angew. Makromol. Chem.*, **122,** 61 (1984).
27. S. F. Xavier and A. Misra, *Polym. Compos.*, **6,** 93 (1985).
28. S. Y. Hobbs, *Nature Phys. Sci.*, **234,** 12 (1971).
29. R. H. Burton, T. M. Day, and M. J. Folks, *Polym. Comun.*, **25,** 361 (1984).
30. K. Ikeda, *Kobunshi Ronbunshu*, **46,** 45 (1989).
31. D. C. Campbell and M. M. Qayyum, *J. Polym. Sci. Polym. Phys. Ed.*, **18,** 83 (1980).
32. K. Nakamae, N. Shibata, and T. Matsumoto, *J. Adhes. Soc. Jpn.*, **19,** 536 (1983).
33. J. A. Koutsky, A. G. Walton, and E. Baer, *J. Polym. Sci. Polym. Lett. Ed.*, **5,** 177 (1967).
34. L. Klostermann, *Plastverarbeiter*, **33,** 262 (1982).
35. J. Menczel and J. Varga, *J. Thermal Anal.*, **28,** 161 (1983).
36. H. Nakagawa and H. Sano, *Polym. Prepr. Jpn.*, **33**(4), 680 (1984).
37. J. W. Gruner, *Z. Krist.*, **88,** 412 (1934).
38. G. Natta, *Makromol. Chem.*, **35,** 93 (1960).
39. F. Rybnikář, *J. Macromol. Sci. Phys.*, **B19,** 1 (1981).
40. B. Lotz and J. C. Wittmann, *J. Microsc. Spectrosc. Electron.*, **10,** 209 (1985).
41. J. C. Wittmann and B. Lotz, *J. Mater. Sci.*, **21,** 659 (1986).
42. J. A. Koutsky, A. G. Walton, and E. Baer, *J. Polym. Sci. Polym. Lett. Ed.*, **5,** 185 (1967).

*Received October 3, 1989*
*Accepted January 5, 1990*